COMPARATIVE ANALYSIS OF SOME TIRE DEFORMATION MODELS USED FOR THE PREDICTION OF TRACTION CHARACTERISTICS
/
ANALIZA COMPARATIVĂ A UNOR MODELE DE DEFORMARE A PNEULUI ÎN SCOPUL OBŢINERII CARACTERISTICILOR DE TRACŢIUNE

Prof. Ph.D. Stud. Eng. Roşca R.*[1)], Assoc. Prof. Ph.D. Eng. Cârlescu P.[1)], Prof. Ph.D. Eng. Ţenu I.[1)]
[1)] University of Agricultural Sciences and Veterinary Medicine "Ion Ionescu de la Brad" Iaşi / Romania;
Tel: 0232-407561; E-mail: rrosca@uaiasi.ro

Keywords: *tire traction, super-ellipse, traction force*

ABSTRACT

In the present paper the deformation of the tire section is under load is taken into account. The tire section is considered to be elliptical; under load the minor axis decreases, while the major axis increases. The equations of the traction model were incorporated in a computer program; the length, width and area of the contact patch, the traction force and traction efficiency are calculated for each value of the wheel slip.

Field tests were performed in order to validate the model; the experimental data were collected during plowing tests. In order to evaluate the precision of the model the predicted data were compared with the test data by the means of a goodness-of-fit analysis.

REZUMAT

Lucrarea prezintă un model pentru interacţiunea pneu-sol, model care se ţine cont de deformarea secţiunii pneului.Astfel, se consideră că pneul are în secţiune formă eliptică; sub acţiunea sarcinii verticale secţiunea se deformează, păstrându-şi forma eliptică (axa mică se scurtează, iar axa mare se alungeşte). Ecuaţiile pentru modelarea tracţiunii roţii cu pneu au fost introduse într-un program de calculator, care determină, pentru fiecare valoare a patinării roţii, lungimea şi lăţimea petei de contact, forţa de tracţiune şi randamentul de tracţiune.

S-au efectuat teste în camp pentru validarea modelului,datele fiind colectate la efectuarea arăturii. S-a efectuat o analiză a corelaţiei datelor experimentale cu cele oferite de model pentru a valida modelul dezvoltat.

INTRODUCTION

The tire-soil interaction models can be based on empirical, semi-empirical and analytical methods (*Tiwari et al., 2010*).

Empirical methods are mainly based on soil properties (cone index, plate sinkage, shear strength) using similitude and dimensional analysis. At the end of the Second World War, this approach evolved as a means of measuring trafficability of soil at the US Army Corps of Engineers, Waterways Experiment Station (*Tiwari et al., 2010*). The empirical models were developed using traction data recorded from operating vehicles; for some of them, cone index, measured with a standard cone penetrometer, was the only soil property taken into account. Wismer and Luth (*1972*) developed a widely used model for bias tyres, based on a soil-tyre numeric, which under-predicted the traction force when applied to radial tyres. The Brixius (*1987*) equations, as a refinement of the Wismer and Luth equations, expressed the gross traction ratio (GTR) as a function of slip and wheel mobility number, using a curve fitting technique in order to evaluate the coefficients for the traction equation (*Lee et al.,2016*).

The semi-emipirical models represent a physical-based approach, which considers the mechanics of the wheel-soil interaction and are suitable for practical applications (*Battiato and Diserens, 2017*). In the semi-empirical models, the shear deformation of soil is considered; the models are based on soil parameters obtained by the means of a bevameter technique (penetration and shear tests), assuming that the vertical deformation of soil is similar to the deformation under a sinking plate, while the shear deformation of soil under a traction device is similar to the shear action of a torsion device (*Tiwari et al., 2010*). The parameters involved in the equations are determined experimentally. For agricultural soils, the Janoshi and Hanamoto (*1961*) equation is one of the most frequently used.

The analytical models are formulated using elasticity and plasticity approaches. Elasticity models are based on the classical mechanical contact theory in order to predict deformations and stresses (using, for example, the Boussinesq's approach), while plasticity based models take into account material (soil) failure

theories. Despite the rather sophisticated theoretical base of these models, there are authors (*Upadhya et al. 1990; Xia, 2011*) who concluded that analytical models never adequately describe the interaction between tyre and soil due to the large number of soil parameters that should be taken into account and to their variability

The tire-soil interaction models are used in order to predict the wheel traction force and traction efficiency. Besides these, they also take into account the shape and area of contact patch between tire and soil, which is also used for the calculation of the surface pressure and is also considered by the models for stress propagation in soil and for the prediction of the compaction risk (*Diserens et al., 2011*).

In a previous paper (*Roşca et al., 2014*) a semi-empirical model for predicting the traction force and traction efficiency was presented; the model was applied on a 2WD agricultural tractor, assuming that the shape of the tire-ground contact area is a super ellipse. The model assumed that the super ellipse equation describes the shape of the tire-ground contact surface and was considered to be a reasonable compromise between the more simple empirical models, for which the range of applicability is limited to the cases having similar conditions to the ones from which the models were derived, and the analytical models, which require in-situ evaluation of a large number of soil properties. Experimental results from plowing tests were used in order to validate and verify the applicability of the model, using a goodness-of-fit analysis. For the case of the traction force, the value of the Pearson r^2 correlation coefficient achieved values between 0.921 and 0.925, thus confirming the validity of the model; for the case of traction efficiency lower values of the Pearson coefficient were obtained, due to the lower values predicted by the model at wheel slips bellow 15%.

One of the key elements of the above mentioned model was the tire change in volume due to deflection under load, which was calculated considering that the tire radius increases as the tire flattens in the contact area; the tire width was considered constant.

In order to improve the theoretical results regarding the wheel traction efficiency in the present paper the deformation of the tire section was also taken into account. The tire section was considered to be elliptical; under the vertical load the minor axis decreased, while the major axis (tire width) increased.

MATERIAL AND METHODS

The tire-soil interaction model is based on the one developed earlier (*Roşca R. et al., 2014*) and its schematics is shown in fig. 1: under the vertical load (G), the wheel sinks into the soil, reaching the depth (z_c) and the load induces tyre deflection (z_p); as a result, the radius of the contact patch becomes r_d ($r_d > r_0$), and the length of the contact patch is:

$$l_c = 2 \cdot r_d \cdot \sin\beta = 2 \cdot r_0 \cdot \sin\alpha \,. \tag{1}$$

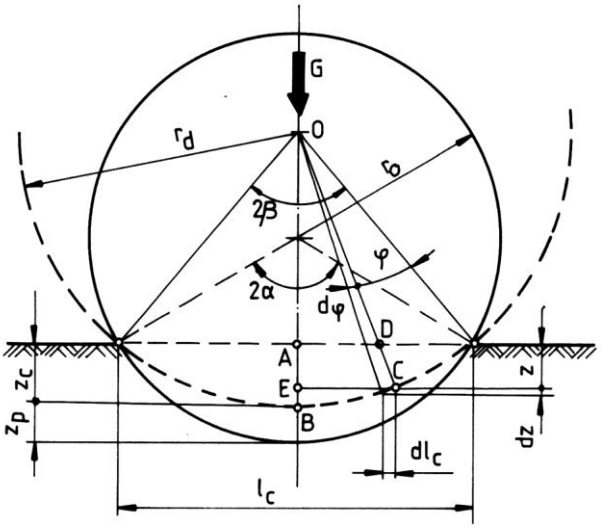

Fig. 1 – Schematics of the wheel-soil interaction model

The shape of the contact patch is assumed to be a super ellipse (*Keller, 2005*):

$$\left(\frac{2 \cdot x}{l_c}\right)^k + \left(\frac{2 \cdot y}{l_w}\right)^k = 1 \,, \tag{2}$$

where k is the super ellipse exponent, the minor axis of the super ellipse is assumed to be equal to the tyre width b (Keller, 2005) l_c is the major axis of the super ellipse (length of the contact area) and l_w is the minor axis of the super ellipse (width of the contact area).

The tire-soil pressure was defined using the pressure-sinkage relationship:

$$p = k \cdot z^n, \tag{3}$$

where p is the normal pressure [kPa], z is the deformation [m], and k [kPa/m^n] and n are constants.

Based on the tire-soil pressure and assuming that the tire is perfectly elastic (*Ghiulai and Vasiliu, 1975*) finally leads to:

$$G = \int_0^{2\beta} p \cdot b(\varphi) \cdot r_d \cdot \cos(\beta - \varphi) \cdot d\varphi = q_p \cdot \Delta V_p, \tag{4}$$

where φ is the current angle, defining the position along the contact surface, p is the normal pressure, q_p is the tyre volume stiffness and ΔV_p is the tyre change in volume due to deflection.

In the initial paper (*Roşca et. al., 2014*) the tire change in volume due to deflection ΔV_p was evaluated considering that the tire radius increases from r_0 to r_d as the tire flattens in the contact area, while the tire width was considered constant (fig. 2).

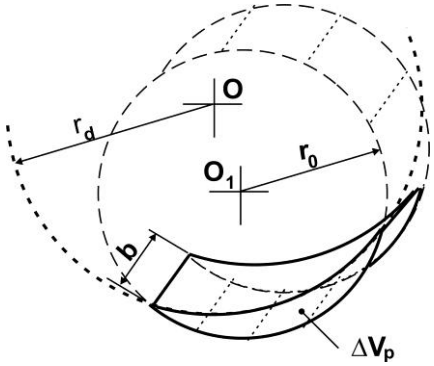

Fig. 2 - Initial tire deformation model

ΔV_p - tyre change in volume due to deflection;
b - tire width;
r_0 – radius of the undeflected tire;
r_d – radius of the contact patch under vertical load.

Finally, after several transformations of equation (4), the following equation is obtained:

$$k \cdot \int_0^{2\beta} b(\varphi) \cdot r_d^{n+1} \cdot [\cos(\beta - \varphi) - \cos\beta]^n \cdot \cos(\beta - \varphi) \cdot d\varphi + \frac{4}{3} \cdot b \cdot q_p \cdot \beta^3 \cdot r_d^2 = \frac{4}{3} \cdot b \cdot q_p \cdot \alpha^3 \cdot r_0^2. \tag{5}$$

In the present study the deformation of the tire cross-section is considered; the shape of the tire cross-section is approximated by an ellipse (*Koutný, 2007*), as shown in fig. 3a. Under the effect of vertical load (G, fig. 1), the cross-section is deformed, but the elliptical shape is preserved (fig. 3b): the minor semi-axis decreases and becomes h-z_p, while the major axis increases from b (tire width in the unloaded condition) to l_w.

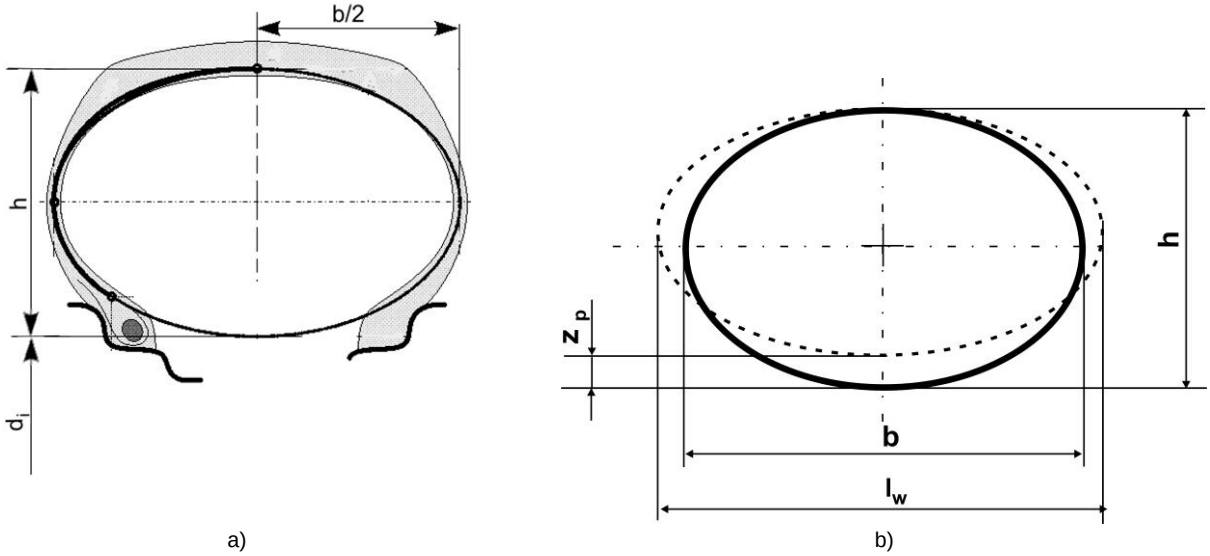

a) b)

Fig. 3 – Model for tire section deformation

a) tire section prameters; b) tire section deformation under load;
d_i – rim diameter; h – tire section height; b-tire width (undeformed); l_w – tire width (under load); z_p - tire deflection under vertical load

The major axis of the ellipse is calculated assuming that its perimeter remains constant:

$$2\pi \cdot \sqrt{\frac{(b/2)^2 + (h/2)^2}{2}} = 2\pi \cdot \sqrt{\frac{(l_w/2)^2 + [(h - z_p)/2]^2}{2}}, \quad (6)$$

which results in:

$$l_w = \sqrt{b^2 + 2 \cdot h \cdot z_p - z_p^2}\ . \quad (7)$$

The tire volume change ΔV_p is calculated as the cross-section area multiplied by the length of the contact patch, resulting in:

$$\Delta V_p = 2 \cdot \alpha \cdot r_o \cdot \pi \cdot \frac{b}{2} \cdot \frac{h}{2} - 2 \cdot \beta \cdot r_d \cdot \pi \cdot \frac{l_w}{2} \cdot \frac{h - z_p}{2} = 0{,}5 \cdot \pi \cdot \left[\alpha \cdot r_0 \cdot b \cdot h - \beta \cdot r_d \cdot l_w \cdot (h - z_p)\right]. \quad (8)$$

After several transformation 4quation (4) becomes:

$$k \cdot \int_0^{2\beta} b(\varphi) \cdot r_d^{n+1} \cdot [\cos(\beta - \varphi) - \cos\beta]^n \cdot \cos(\beta - \varphi) \cdot d\varphi = q_p \cdot 0{,}5 \cdot \pi \cdot \left[\alpha \cdot r_0 \cdot b \cdot h - \beta \cdot r_d \cdot l_w \cdot (h - z_p)\right] \quad (9)$$

The following equations are also obtained from fig. 1:

$$z_c = r_0 - z_p - r_0 \cdot \cos\alpha\,, \quad (10)$$

$$z_p = r_0 \cdot (1 - \cos\alpha) - r_d \cdot (1 - \cos\beta), \quad (11)$$

where z_p is tyre deflection under vertical load.

A computer program is used in order to solve the systems of equations (1), (5), (10), (11) and (1), (9), (10), (11), respectively. The program displays the following values (fig. 4):

- length of the contact patch, l_c;
- width of the contact patch, l_w;
- area of the contact patch;
- calculated value of tire deformation under load, z_p;
- tire sinkage, z_p;
- dynamic radius of the wheel, r_d;
- angle of the contact patch, β;
- maximum shear stress, τ_{max};
- normal pressure, p.

The values of slip, traction force and traction efficiency are saved in a file.

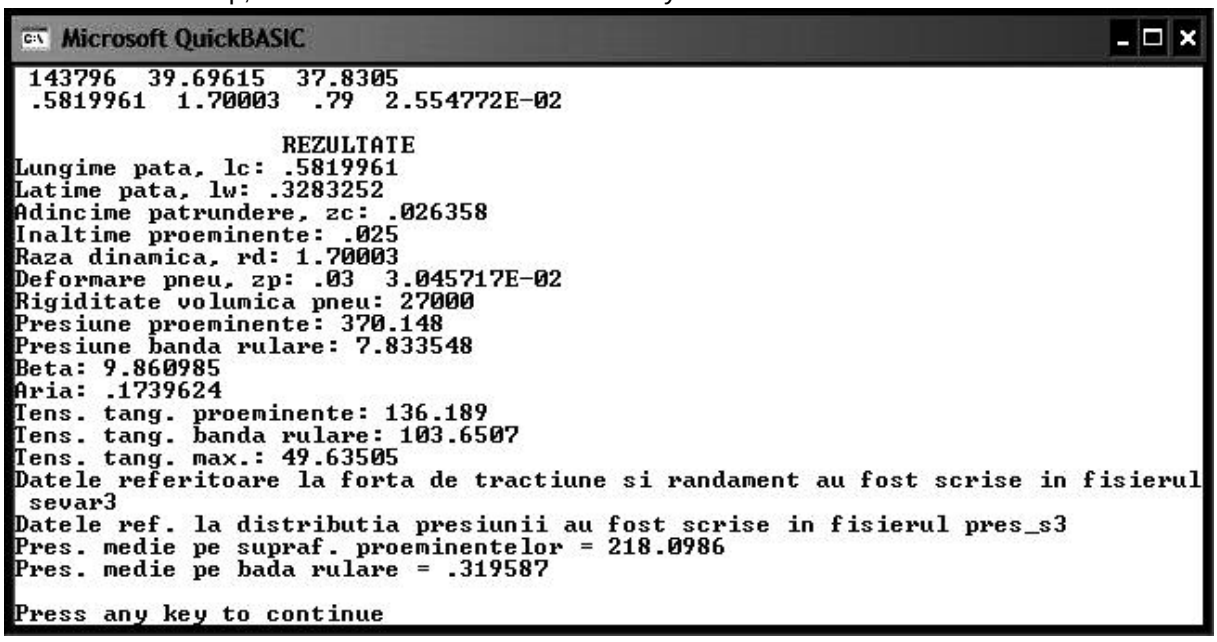

Fig. 4 – Output screen of the computer program

In order to evaluate the maximum traction force it is assumed that it is limited only by the soil shear strength; the Mohr-Coulomb equation is used to calculate the soil maximum shear stress:

$$\tau_{max} = c + p \cdot tg\gamma, \tag{12}$$

where c is soil cohesion [kPa], p is the vertical pressure [kPa] and γ is the internal friction angle.

Soil shear tension was calculated using the Janosi and Hanamoto (1961) equation:

$$\tau = \tau_{max} \cdot \left(1 - e^{-\frac{J}{K}}\right), \tag{13}$$

where K is the soil shear deformation modulus and J is the shear displacement.

The maximum traction force was calculated as the product of shear stress and shear area; according to ASAE S296, the net traction force is $F_N = F_t - R_r$, with the wheel rolling resistance R_r being calculated with the relation (*Elwaleed et al., 2006*):

$$R_r = G \cdot \left(\frac{1}{B_n} + 0.04 + \frac{0.5 \cdot s}{\sqrt{B_n}}\right) \quad [kN]. \tag{14}$$

The wheel numeric B_n is (*ASAE D497.7, 1999*):

$$B_n = \frac{CI \cdot b \cdot d}{G} \cdot \left(\frac{1 + 5 \cdot \frac{z_p}{h}}{1 + 3 \cdot \frac{b}{d}}\right), \tag{15}$$

where CI is the soil cone index [kPa], $d = 2 \cdot r_0$ [m] and h is the tyre section height [m].

The same standard defines the traction efficiency as:

$$\eta_{tr} = (1 - s) \cdot (1 - R_r / F_t). \tag{16}$$

The model was applied to the driving wheel of an U-650 agricultural tractor; the main characteristics of the wheel are presented in table 1.

Table 1

Main characteristics of the driving wheel

Item	Value
Load on the driving tire, G [kN]	11.75
Type of tire	14.00-38
Rim diameter, d_i [m]	0.965
Section height, h [m]	0.307
Exterior diameter of tire, $d_i + 2 \cdot h$ [m]	1.58
Tire width, b [m]	0.370
Tire inflation pressure [kPa]	100

The experimental data were collected during the field tests performed with the U650+P2V plowing unit; the tractor was fitted with a dynamometric frame and an electronic dynamometer, as shown in fig. 5. The plough was mounted on the dynamometric frame and thus the net traction force $F_{t,ef,r}$ was measured directly. During these tests drive wheel slip did not exceed 30% because of the restraints imposed by the plowing process. Different traction forces and drive wheel slips were achieved by changing the operating width and depth of the plough. The traction force for each experimental point was calculated as the average value of nine measurements; the standard error and 95% confidence interval were then evaluated. The experimental results taken into account for the goodness-of-fit analysis are shown in table 2.

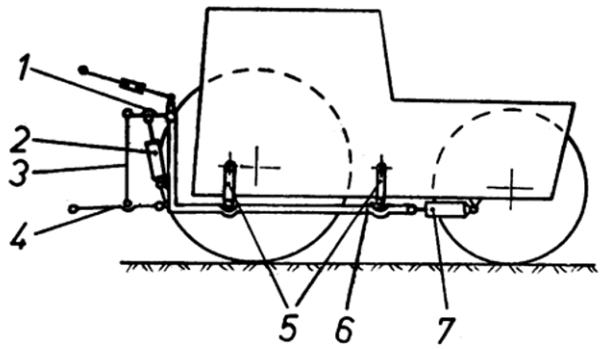

Fig. 5 – Dynamometric frame mount

(Roşca R. et al., 2014)

1,3,4-lifting arms;
2-hydraulic lifting cylinder;
5-frame arms;
6-dynamometric frame;
7-force transducer.

Table 2

Experimental data for traction force

Wheel slip [%]	Average traction force [kN]	Standard error	95% data confidence interval
6	1.8033	0.095	0.2179
9	2.3744	0.116	0.2684
14	3.1033	0.082	0.1891
17	3.3067	0.121	0.2797
18	3.6855	0.116	0.2680
20	4.3122	0.175	0.4029
25	4.6777	0.087	0.2003
26	4.7567	0.114	0.2636
29	5.8800	0.141	0.3249

The tests were performed on wheat stubble sandy loam soil, after cereal harvesting; soil characteristics in the test field are presented in table 3.

Table 3

Characteristics of the test soil

Item		Value
Soil type		Sandy loam soil
Average bulk density [kg/m^3]		1280
Average soil water content [%]		9.5
Soil deformation modulus, K [m]		0.05
Coefficients for the pressure-sinkage equation	k	55
	n	1.3
Soil cohesion, c [kPa]		25
Angle of internal friction, γ [^{0}]		32
Cone penetrometer index, C [kPa]		970

In order to evaluate the goodness-of-fit between model and experimental data the following criteria were considered (*Schunn and Wallach, 2005*):

- percentage of points within 95% confidence interval of data (Pw95CI) – represents the percentage of model predictions that lie within the 95% confidence interval of each corresponding experimental data point;
- mean absolute deviation (MAD) – represents the mean of the absolute value of the deviation between each model point and the corresponding experimental point:

$$MAD = \frac{\sum_{i=1}^{n} |m_i - d_i|}{n}, \tag{17}$$

where m_i is the model mean for point I, d_i is the experimental data mean for point I and n is the total number of points being compared;

- root mean squared deviation (RMSD):

$$RMSD = \sqrt{\frac{\sum_{i=1}^{n} (m_i - d_i)^2}{n}}; \tag{18}$$

- mean scaled absolute deviation (MSAD):

$$MSAD = \sum_{i=1}^{n} \frac{|m_i - d_i| \cdot \sqrt{n_i}}{n \cdot s_i}, \tag{19}$$

where n_i is the number of values contributing to each experimental data mean d_i (n_i = 9) and s_i is the standard deviation for each data mean. A MSAD value of 1.5 means that, on average, the model is 1.5 standard errors off from the experimental data.

- Pearson correlation coefficient r^2.

RESULTS

For the both tire section deformation models the calculations were performed using the same value for the super ellipse coefficient (k=3.5). Table 4 presents some comparative results given by the tire – soil

computer simulation; the assumption that the tire cross-section has an elliptical shape and is deformed due to the vertical load of the tire had the following consequences:

- while the length of the contact patch decreased slightly (from 0.533 m to 0.531 m), the width of the contact patch, l_w, increased from 0.3 m to 0.319 m, resulting in a larger area of the contact surface (0.154 m^2);
- the tire radius r_d decreased from 1.4 m to 1.371 m; as the length of the contact patch did not change significantly, the centre angle β increased from 10.916^0 to 11.19^0;
- the maximum shear stress decreased from 53.3 kPa to 52.01 kPa due to the increase of the contact surface area.

Table 4

Model results

Item	Initial tire deformation model (b const.)	Modified tire deformation model (b elipse)
Length of the contact patch, l_c [m]	0.533	0.531
Width of the contact patch, l_w [m]	0.300	0.319
Tire deflection, z_p [m]	0.02	0.02
Sinkage depth, z_c [m[	0.027	0.027
Area of the contact surface, A_t [m^2]	0.145	0.154
Tire radius, r_d [m]	1.400	1.371
Centre angle of the contact patch, β [^{0}]	10.916	11.19
Maximum shear stress, τ_{max} [kPa]	53.3	52.01

Fig. 6 and 7 present the predicted and experimental results concerning the traction force and traction efficiency. The charts clearly show that the model predicted higher values of the traction force and traction efficiency when the deformation of the tire cross section was considered, due to the increased value of the contact surface area.

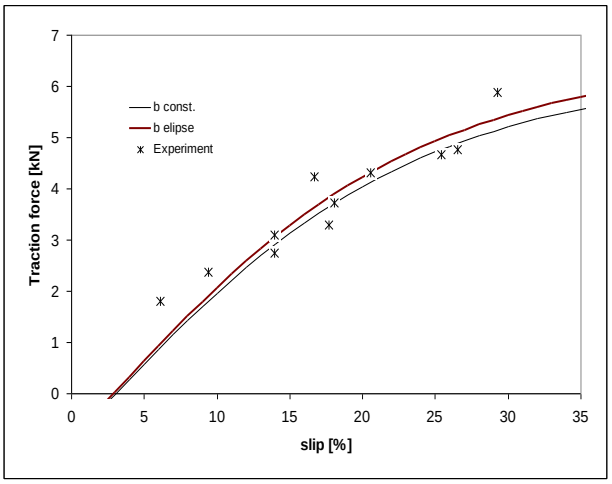

Fig. 6 – Results concerning the traction force

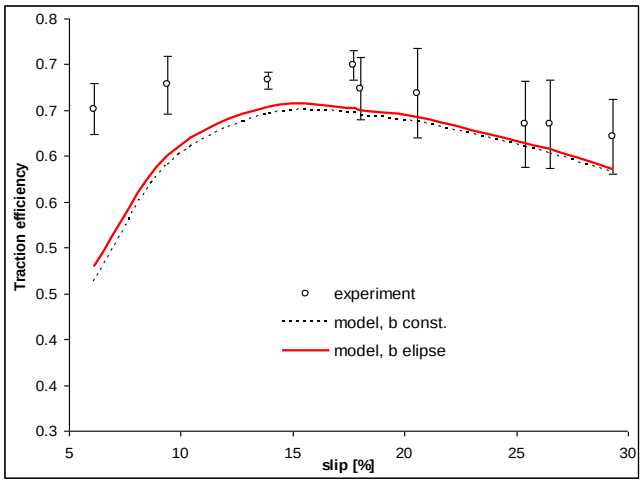

Fig. 7 – Results concerning the traction efficiency

The results of the goodness-of-fit analysis are shown in table 5. Compared to the previous model, the most significant differences were recorded for the traction efficiency: the Pearson correlation coefficient r^2 increased from 0.186 to 0.216, the mean absolute deviation (MAD) decreased form 0.058 to 0.051, root mean squared deviation (RMSD) decreased form 0.0752 to 0.0686 and the mean scaled absolute deviation (MSAD) decreased from 5.225 to 4.557.

Table 5

Goodness-of-fit comparative analysis

Item	Traction force		Traction efficiency	
	Constant cross-section	Deformable cross-section	Constant cross-section	Deformable cross-section
r^2	0.923	0.924	0.186	0.216
PW95CI	66.7	55.6	55.6	55.6
MAD	0.354	0.356	0.058	0.051
RMSD	0.480	0.438	0.0762	0.0686
MSAD	3.122	3.065	5.225	4.577

When referring to the values of the traction force, all the goodness-of-fit parameters recorded better values for the modified traction model, excepting the percentage of points within 95% confidence interval of data (Pw95CI), which has slightly decreased (from 66.7% to 55.6 %).

CONCLUSIONS

A modified semi-empirical model for the prediction of traction performance of a tractor driving wheel is presented in this study. The model assumed that the super ellipse equation describes the shape of the tire-ground contact surface.

The model is a reasonable compromise between the more simple empirical models, for which the range of applicability is limited to the cases having similar conditions to the ones from which the models were derived, and the analytical models, which require in-situ evaluation of a large number of soil properties.

Experimental results from plowing tests were used in order to validate and verify the applicability of the model, by the means of a goodness-of-fit analysis. The analysis showed that the modified traction model provided more accurate results regarding the traction force and traction efficiency then the initial one.

REFERENCES

[1] Battiato A., Diserens E., (2017), Traction performance simulation on differently textured soils and validation: A basic study to make traction and energy requirement accessible to practice, *Soil&Tillage Research*, Vol. 166, pp. 18-32;

[2] Brixius W. W., (1987), Traction prediction equations for bias ply tyres, *ASAE Paper* 87-1622, St. Joseph, Michigan/USA;

[3] Diserens E., Défossez P., Duboisset A., Alaoui A., (2011), Prediction of the contact area of agricultural traction tyres on firm soil, *Biosystems engineering*, Vol. 110, pp. 73-82;

[4] Elwaleed A.K., Yahya A., Zohadie M., Ahmad D., Kheiralla, A.F., (2006), Effect of inflation pressure on motion resistance of a high-lug agricultural tyre, *Journal of Terramechanics*, Vol. 43, pp. 69-84;

[5] Ghiulai C., Vasiliu Ch., (1975), *Ground vehicles dynamics* (*Dinamica autovehiculelor)*, Didactics and Pedagogy Publishing House, Bucharest/Romania;

[6] Janosi Z., Hanamoto B., (1961), The analytical determination of drawbar pull as a function of slip, for tracked vehicles in deformable soils. *Proceedings of the 1st Intl. Conference Mech. Soil-Vehicle Systems*. Turin/ Italy;

[7] Koutný F., (2007), *Geometry and mechanics of pneumatic tires,* Zlin, CZE (available at: http://wanderlodgegurus.com/database/Theory/TireGeometry.pdf);

[8] Lee J.W., Kim J.S., Kim K., (2016), Computer simulations to maximise fuel efficiency and work performance of agricultural tractors in rotovating and ploughing operations, *Biosystems Engineering*, Vol. 142, pp. 1-11;

[9] Keller T., (2005), A model for prediction of the contact area and the distribution of vertical stress below agricultural tyres from readily available tyre parameters, *Biosystems Engineering*, Vol. 92, no.1, pp.85-96;

[10] Roşca R., Cârlescu P., Ţenu I., (2014), A semi-empirical traction prediction model for an agricultural tyre, based on the super ellipse shape of the contact surface, *Soil&Tillage Research*, Vol. 141, pp.10-18;

[11] Schunn C.D., Wallach D., (2005), Evaluating goodness-of-fit in comparison of models to data. *Psychologie der Kognition: Reden and Vorträge anlässlich der Emeritierung*, pp. 115-154, W. Tack (Ed.), University of Saarland Press, Saarbrueken, Germany,

[12] Tiwari V.K., Pandey K.P., Pranav P.K., (2010), A review on traction prediction equations, *Journal of Terramechanics*, Vol.47, pp.191-199;

[13] Upadhyaya S. K., Wulfson D., Jubbal G., (1990), Review of traction prediction equations. *ASAE Paper 90 – 1573*, St. Joseph, Michigan;

[14] Xia K., (2011), Finite element modeling of tire/terrain interaction: Application to predicting soil compaction and tire mobility, *Journal of Terramechanics*, Vol. 48, pp. 113-123;

[15] *** ASAE D497.7, (1999), *Agricultural Machinery Management Data*. St. Joseph, Michigan, U.S.A.